DOI: 10.21062/mft.2023.022 http://www.journalmt.com

Investigation and Measurement of Nanomechanical Properties of the HSS Powder Metallurgy ASP2017 and ASP2055 Steels

Jana Escherová, Juraj Majerský (0000-0003-2342-0852)[1], Jozef Majerík (0000-0002-6577-1987), Igor Barényi (0000-0002-9296-600X), Henrieta Chochlíková
Faculty of Special Technology, A. Dubcek University of Trencin. Ku kyselke 469, 911 06 Trencin. Slovakia. E-mail: jana.escherova@tnuni.sk, juraj.majersky@tnuni.sk jozef.majerik@tnuni.sk, igor.barenyi@tnuni.sk, henrieta.chochlikova@tnuni.sk

This article deals with the analysis of selected structural components of the HSS powder metallurgy steel ASP 2017 and ASP 2055 by quasi-static nanoindentation analysis. The microstructure and nanomechanical properties (reduced modulus of elasticity, nanohardness) of base material are analysed. The selected structural components based on the analysis of microstructure were investigated by the nanoindentation. The purpose was to describe basic condition of the structure and local nanomechanical properties of tested materials. Obtained results will serve as basic values for comparing the properties of modified states of those steels. Triboindenter Hysitron TI950 Triboindenter was used for research by using nanoindentation and built-in microscopy. Indentation tip with Berkovich geometry eas used for the experiment. The measured data were then analysed and evaluated by the Triboscan evaluation software.

Keywords: Quasi-static nanoindentation, Nanohardness, Reduced Young's modulus, Powder metallurgy steels, Microstructure

1 Introduction

The investigated tool steels produced by powder metallurgy are characterized by special material and technological properties, as well as their use in practice on highly stressed components of special technique, in order to increase their useful properties and prolong their service life. In the experiment two types of high-speed steels called ASP 2017, ASP 2055 were used produced by powder metallurgy. In the industry the ASP 2017 and ASP 2055 steel can be found in many applications, for example cutting tools or high-performance tools. The aim of this research was to describe the basic condition of the structure and local nanomechanical properties via quasistatic nanoindentation method. Through this method, authors of this article evaluated the Young's modulus of elasticity and nanohardness on the experimental samples. In the production of various components, a relatively large number of tool steels are used in industrial practice, which are exposed to high stresses and wear during friction processes throughout operation which have a great impact on their lifetime. The aim of nanoindentation tests is to determine the modulus of elasticity and hardness of the sample material from load and displacement measurements. Nanoindentation hardness tests are usually performed by spherical or pyramid test tips [1, 2, 3, 4]. Measurement by the quasi-static nanoindentation method requires the penetration of a Berkovich geometry test tip into the sample under the specified load and displacement control. The displacement (h) is monitored as a function of the load (P) during the whole load-unload cycle, where the P-h relation is known as the nanoindentation curve (Fig. 3) [1, 2, 3]. Special characteristics of performed indents were described in the study of the authors Naimi-Jamal and Kaupp [5]. For this reason, many studies were realized by using of nanoindentation. This topic – nanomechanical properties of the tool steels was researched by various teams of authors [6, 7, 8, 9, 10, 11, 12]. Boumali et al. [12] in their study carried out an experiment by using the quasi-static nanoindentation, which was carried out on layers of the tool steel AISI H13. The Hysitron TI 950 triboindenter experimental device with a Berkovich geometry test tip was used in the experiment, i.e.., with the same conditions as the research provided in this article. Figures 1a. b [12] shows the nanoindentation curves of two borided samples. Three performed indents in each region (FeB, Fe2B and also in transition zone) were done at the cross-sections of the treated experimental samples to determine the numerical values of reduced Young modulus and the corresponding values of nanohardness [12]. Figures 2a, b shows the indentation points on the surfaces of FeB and Fe2B zones along the cross-section of tested AISI H13 steel

at 1000 °C for 4 and 6 hours. The data from Figures 1a. b were used to calculate the values of reduced Youngs modulus of elasticity and nanohardness, too [12].

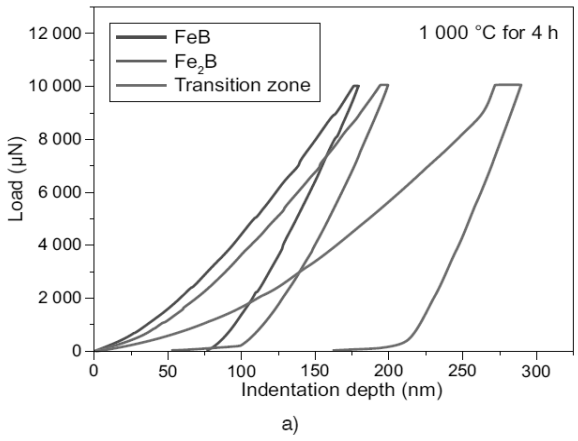

Fig. 1a *Curves of nanoindentation tests for the boronized AISI H13 steels at 1000 °C for two exposure times: a) 4 h [12]*

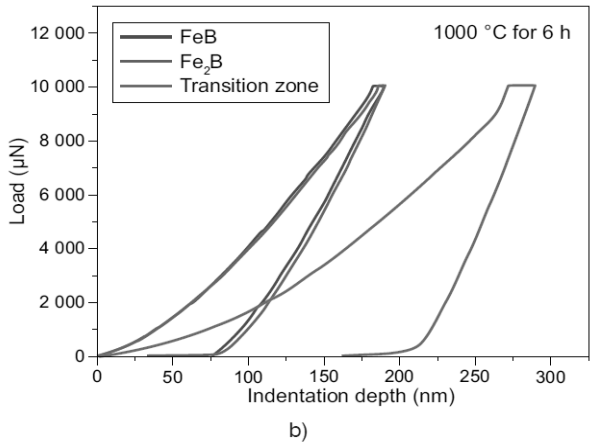

Fig. 1b *Curves of nanoindentation tests for the boronized AISI H13 steels at 1000 °C for two exposure times: b) 6 h [12]*

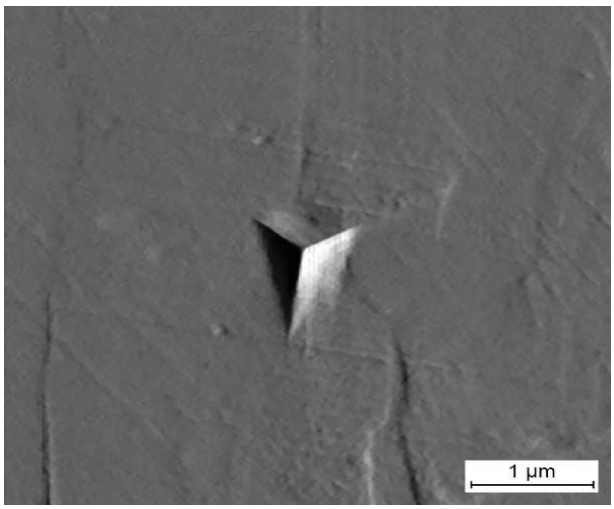

Fig. 2a *SPM scan of the indented surface of AISI H13 tool steel in two different locations at 1000 °C for two exposure times: a) 4 h [12]*

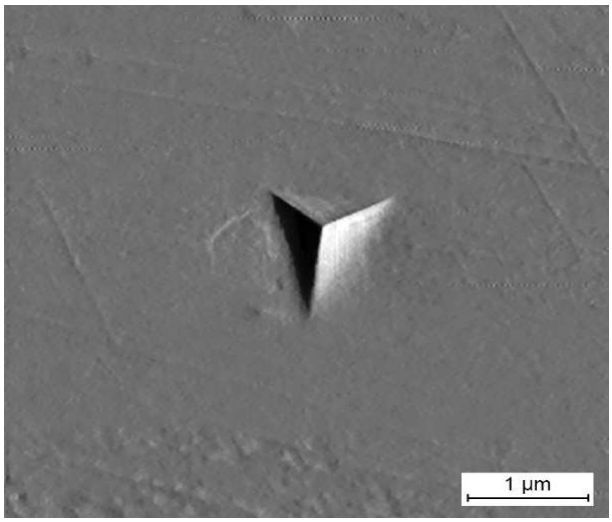

Fig. 2b *SPM scan of the indented surface of AISI H13 tool steel in two different locations at 1000 °C for two exposure times: b) 6 h [12]*

Nanoindentation analysis can also be used for a wide range of investigations, especially for metallic materials with specific properties, or their alloys. This fact is also documented by several studies and research of teams of authors of this issue [13 -22]. In addition to nanoindentation analysis of the basic material structure, the authors' research also focused on the analysis of individual layers or coatings applied by PVD or CVD deposition [23 - 25]. Hernández at al. [26] investigated optical and tribo-mechanical characteristics in metal-ceramics multilayer coatings with using mentioned method. Paul et al. [27] researched local deformation behaviour of the copper harmonic structure near grain boundaries through nanoindentation. Ohmura et al. [28] solved the pop-in phenomenon as a fundamental plasticity probed also by nanoindentation technique. Some other special nanomechanical applications, like composite wires were solved by Xiang et al. [29].

2 Experimental details for high-speed steels ASP2017 and ASP2055

As a part of the presented research, optical and electron microscopy was applied in order to monitor the microstructure. Furthermore, an experimental method called quasi-static nanoindentation was used. An optical microscope Neophot 32 equiped by Canon digital camera, were used to examine the microstructure. Electron microscopy was performed using a Tescan MIRA device. Quasi-static nanoindentation, in addition to measuring the nanohardness *H* [GPa], also measures and evaluates the reduced Young's modulus of elasticity *Er* [GPa]. Their use is in areas where the mentioned quantities cannot be measured by conventional methods of measuring mechanical properties. Nanoindentation analysis in its essence is referred to as a contact

method. Quasi-static nanoindentation measurement requires impressing a test tip into the sample under a specified load or displacement control. Quasi-static nanoindentation measurement requires pressing a Berkovich geometry test tip into the sample under a specified load or displacement control. Displacement (*h*) is monitored as a function of load (*P*) throughout the load-unload cycle, where the *P-h* dependence is known as the nanoindentation curve. Nanoindentation analysis was performed by a Hysitron Triboindenter TI 950 device.

2.1 Characteristics of tested materials

As a part of the experiment two types of high-speed steels ASP 2017 and ASP2055 were used. These high-speed steels are produced by the process of powder metallurgy. The ASP 2017 type steel belongs to high-speed steels group, which are very tough with excellent grindability, suitable for the screw-cutting taps, bimetallic saws or roughing cutters and so on. The ASP 2055 type steel belongs to highly alloyer high-speed steels group with very fine carbide structure. These types of steels are suitable for the production of shaping and face milling cutters, taps or various high-performance tools for cold work and so on. Both of these steels should be processed by a machining. It means grinding, turning, milling, further fine grinding, electro-erosive machining, welding, various special methods with preheating. The chemical composition of both steels is mentioned in Table 1 and mechanical properties in Table 2.

Tab. 1 *Chemical composition of ASP 2017 and ASP 2055 steels*

Chemical composition HSS steel ASP2017							
C	Cr	Mo	W	Co	V	Nb	Fe
0.80	4.0	3.0	3.0	8.0	1.0	1.0	balance
Chemical composition HSS steel ASP2055							
C	Cr	Mo	W	Co	V	Nb	Fe
1.69	4.0	4.6	6.3	9.0	3.2	2.1	balance

Tab. 2 *Mechanical properties of ASP 2017 and ASP 2055 steels*

Mechanical properties of investigated tool steels						
Yield $R_{p0,2}$ [MPa]	Tensile R_m [MPa]	Impact KV/KU [J]	Elongation A [%]	Reduction in cross section on fracture Z [%]	As-Heat-Treated Condition	Brinell hardness [HBW]
Steel ASP2017						
191 (≥)	423 (≥)	43	11	41	Solution and Aging, Annealing, Ausaging, Q+T,etc	211
Steel ASP2055						
192 (≥)	435 (≥)	23	21	43	Solution and Aging, Annealing, Ausaging, Q+T,etc	424

2.2 Experimental method, the quasi-static nanoindentation

In order to perform an experiment for individual measurements, the method called quasi-static nanoindentation was used. In other literatures we can also meet with the term nanoindentation analysis [1 - 3]. Used testing method for HSS steels type ASP 2017 and ASP 2055 was realised by the device Hysitron TI 950 Triboindenter. Quasi-static nanoindentation analysis was performed on prepared metallographic samples and then evaluated by Triboscan software. Quasi-static nanoindentation was realized in the laboratory focused on surface microanalysis and testing of local mechanical properties of materials. The experimental testing with the Berkovich indentation geometry was realized at standard room temperature 20 °C. When measuring by the method mentioned above, the resulting load as well as the displacement were determined in the measurement process. During the process, the Berkovich geometry of indentation tip was gradually pressed into the material surface according to standard *P-h* profile (Fig. 4). The nanoindentation was realised at predetermined points (Figs. 7, 8). These points were selected on the scanned surface obtained by the SPM method (according to Figs. 2a, b from sources) directly from the original microstructure. All measurements of this investigation were investigated by the light microscopy LO, which is part of the equipment Hysitron Triboindenter TI 950. The next point of this research is a determination of SPM scans (Figs. 7, 8)

of the selected area with the selected dimensions 20x20 and 10x10 μm. This is the selection of indents, which were defined by a manual way based on a predetermined number of indents in the material area of each sample. Standard trapezoid was used as the loading curve (Fig. 4a) for the first measurement with a maximum of 5000 μN during the duration of the indentation t = 2 s and for the second measurement also with a maximum of 5000 μN with the time t = 2 s. An illustration of the investigated points of the formed places on the SPM scan for the material of high-speed steels of types ASP 2017 and ASP 2055 is shown in (Figs. 7, 8). Numerical values of the reduced Young's modulus of elasticity *Er* and nanoindentation hardness *H* [GPa] thus obtained in their specific positions were simultaneously evaluated using Triboscan software. The values of *Er* and *H* for a specific type of steel are shown in Tab. 4 and 5., The *P-h* curves for the specific indentation points are generated as a last point at the conclusion after the measurement for the specified indentation points, which can be seen in (Figs. 9, 10).

The fundamental principle of quasi-static nanoindentation method (schematic illustration & principle is described in Fig. 3) can be described via data, which were obtained by load and displacement *P-h* curve. The nanomechanical properties was obtained by indirect way – not by the measuring of the imprint. The loading part of indentation curve should be called elastic-plastic area (Fig. 3 and 4b), while the unloading part of this curve has elastic character. For the determination of the nano-hardness *H* calculation, the indentation depth h_c (Fig. 4c), which is the vertical distance between the indentation tip and the point of maximum indentation depth. This depth can be calculated by next formula:

$$h_c = h_{\max} - h_s = h_{\max} - \varepsilon \frac{P_{\max}}{S} \qquad (1)$$

Where h_s is elastic deformation situated in the indentation area after unloading part of the *P-h* curve. The value ε describes the properties of indenter. Then, the nano-hardness *H* value of the tested specimen can be expressed as:

$$H = \frac{P_{\max}}{A} \qquad (2)$$

Where *A* is defined as a real projected contact area between the specimen surface and indenter. The *A* value can also be calculated directly from h_c and indenter geometry. For determination of Youngs modulus of elasticity *E*, the reduced Youngs modulus of elasticity *Er*, can be then calculated in the following formula:

$$E_r = \frac{\sqrt{\pi}}{2\beta}\frac{S}{\sqrt{A}} \qquad (3)$$

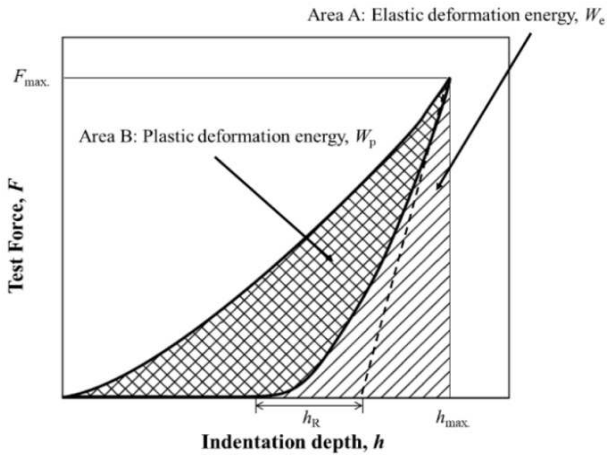

Fig. 3 *Schematic illustration of the plastic and elastic part of the nanoindentation P-h curve [17]*

According to formula (4) mentioned below the calculation of the Young's modulus of elasticity of the *Es* phase was performed for tested ASP 2017 and ASP 2055 high-speed steels.

$$E_s = (1-\upsilon_s^2)/(\frac{1}{E_r} - \frac{1-\upsilon_i^2}{E_i}) \qquad (4)$$

Where υ_s *is* Poisson´s constant of the sample, υ_i is Poisson´s constant for the indenter Berkovich type and E_i represents the test tip modulus. Based on information from suppliers the values were set following: υ_i=0.07, υ_s=0.29 and E_i=1141 GPa.

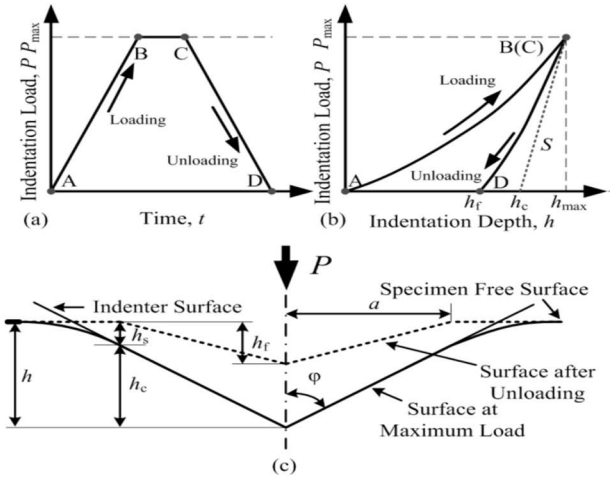

Fig. 4 *Fundamental principle of quasistatic nanoindentation, where a) Load time curve (standard trapezoid), b) Load – displacement P- h curve, c) parameters of indentation process [4]*

These values were used in all calculations. Calculations of Young's modulus of elasticity of the phases E_s for the investigated ASP 2017 and ASP 2055 HSS steels are mentioned below in the article. The obtained values of Young's modulus of elasticity of the phases E_s in HSS steel type ASP 2017 for phases primary carbide, secondary carbide, and matrix (ferrite) are as follows. The calculation of E_s for the

primary carbide phase in ASP 2017 HSS steel is calculated according to Eq. 4. Calculated value for E_r is172.86 GPa. After substituting these values into relationship (Eq. 4), the Young's modulus of elasticity of the phase is Es=186.43 GPa. For the secondary carbide phase of ASP 2017 the value of the Young's modulus of elasticity of the phase Es=185.92 GPa was calculated, the value of the reduced Young's modulus of elasticity was Er=172.46 GPa. The last phase of ASP 2017 is a matrix (ferrite) with calculated numerical value Es=464.95 GPa, and the character of the reduced Young's modulus of elasticity is E_r=351.86 GPa. All values were averaged. In the same way values of Young's modulus of elasticity of the phases E were obtained and calculated$_s$ and reduced Young's modulus of elasticity E_r in ASP 2055. For the primary carbide phase in ASP 2055 steel was reached the value of the Young's modulus of elasticity of the phase E_s=232.45 GPa, where the value of the average reduced Young's modulus of elasticity was Er=207.80 GPa. For the matrix phase (ferrite) in ASP2055 steel is the value of the Young's modulus of elasticity of the phase Es=304.54 GPa and the value of the reduced Young's modulus of elasticity is Er=257.76 GPa. Table 3 shows a comparison of the E_s values and the E_r values.

Tab. 3 *Mutual comparison of measured reduced Young's modulus of elasticity with the calculated Young's modulus of elasticity of examined phase*

Steel	*The steel phase*					
	Primary carbide		*Secondary carbide*		*Matrix (Ferrite)*	
	E_r *[GPa]*	E_s *[GPa]*	E_r *[GPa]*	E_s *[GPa]*	E_r *[GPa]*	E_s *[GPa]*
ASP 2017	*172.86*	*186.43*	*172.46*	*185.92*	*351.86*	*464.95*
ASP 2055	*207.80*	*232.45*			*257.76*	*304.54*

2.3 Microstructural analysis of examined steels

The ASP 2017 steel is supplied in a soft-annealed condition. The structure consists of larger primary carbides and smaller secondary carbides formed during the annealing. Carbides are regularly distributed in the ferritic matrix (see Figs. 5a, b). The ASP 2055 is a steel with very finely evenly distributed carbides in a ferritic matrix. The ASP 2055 steel has high toughness because the formation of secondary carbides is suppressed (see Figs. 6a, b). The microstructural analysis of tested steels was realized through LO, see Figs. 5a, 6a, (Neophot 32) and SEM (Tescan MIRA) microscopy, as can be seen in Figs. 5b, 6b.

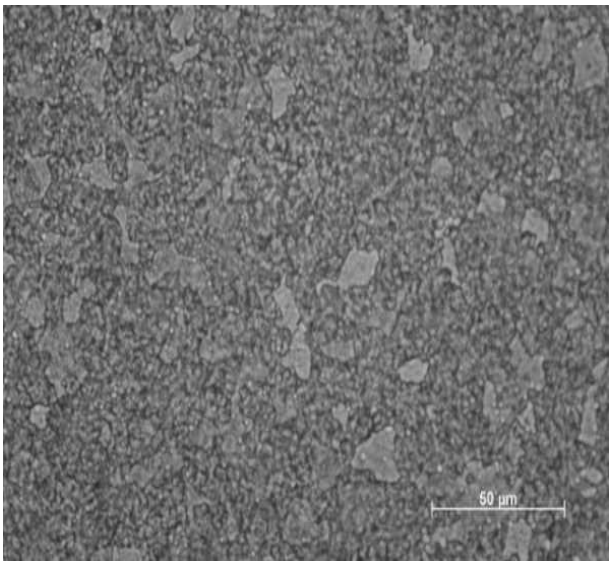

Fig. 5a *LO microstructure of HSS steel ASP 2017*

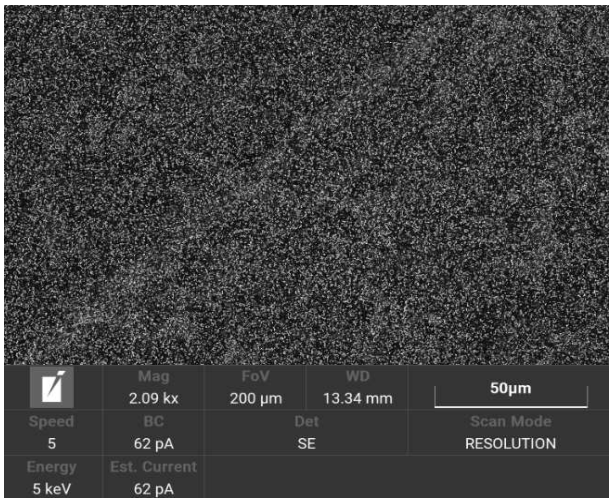

Fig. 5b *SEM microstructure of HSS steel ASP 2017*

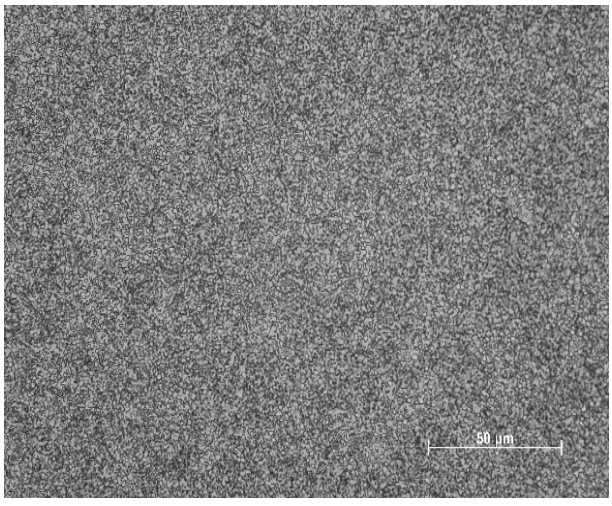

Fig. 6a *LO microstructure of HSS steel ASP 2055*

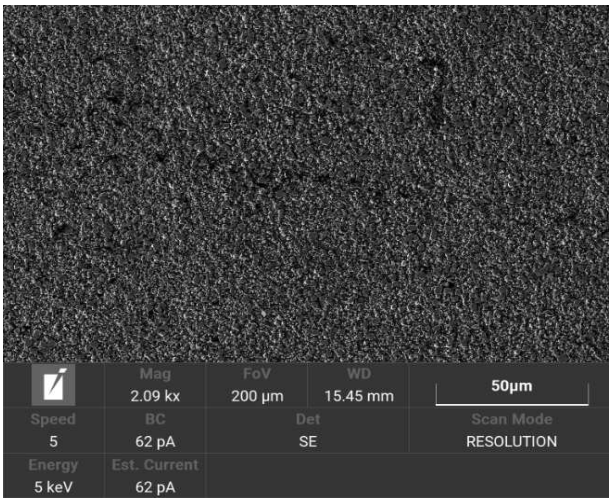

Fig. 6b *SEM microstructure of HSS steel ASP 2055*

3 Results and discussion

Based on experimental testing two measurements were performed which consisted for both types of high-speed steels (ASP 2017 and ASP 2055) from five indents at a designated location of the microstructure of the examined area (Boundary). The examined area for the first performed measurement was bounded by dimensions 20x20 μm (Fig. 7) and for the second experimental measurement the area with dimensions 10x10 μm was measured (Fig. 8). Nanoindentor Hysitron Triboindenter TI 950 placed in the laboratories of the Faculty of Special Technology was used for experimental research. A loading curve in the shape of a regular trapezoid was used for the first and second measurements, the maximum reached value was 5000 μN with a holding time at this of 2 seconds. The measured positions of specific indentations are located on the generated SPM scan of the evaluated area for individual tested metallographic samples from ASP 2017 and ASP 2055 HSS steels (Fig. 7 and Fig. 8). The acquired values of the reduced Young's modulus of elasticity *Er* [GPa] and nanoindentation hardness *H* [GPa] for both types of steel from experimental testing in specific positions are shown in Tab. 4 and Tab. 5. In Tab. 6 we can see the comparison of the phases of HSS steels, their nanohardness and the reduced Young's modulus of elasticity. The final shapes of measured *P-h* curves for both tested steels ASP 2017 and ASP 2055, which were obtained from measured points directly placed on investigated area of the microstructure acquired from both metallographic samples, as can be seen in (Fig. 9 and 10). The designation of specific curves for steels ASP 2017 and ASP 2055 is the same with the designation of investigating points in (Fig. 7 and Fig. 8) and in Tab. 4 and Tab. 5.

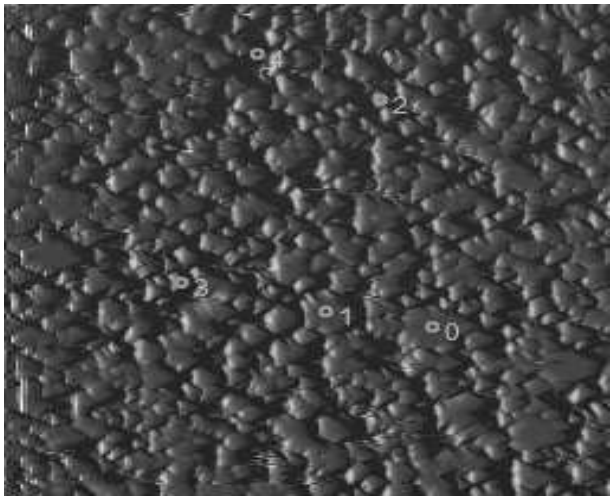

Fig. 7 *SPM scan of ASP 2017(area 20x20) μm*

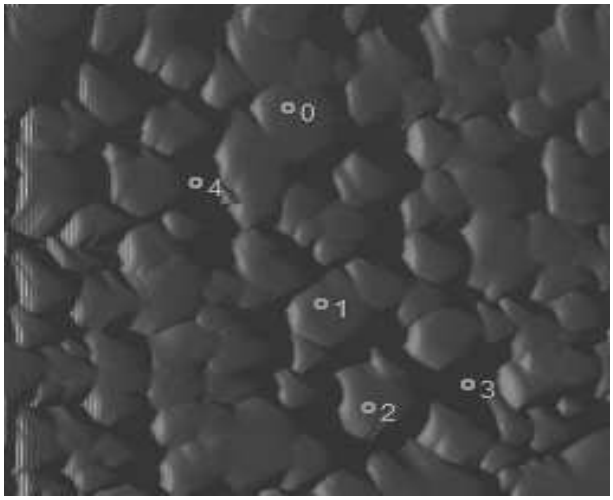

Fig. 8 *SPM scan of ASP 2055 (area 10x10) μm*

Tab. 4 *Mechanical properties of ASP 2017 steel*

Position	Reduced Young's modulus of elasticity E_r [GPa]	Nanohardness H [GPa]	Diameter E_r	Diameter H	Estimated phase
0	162.88	6.41	172.86	6.09	Primary carbide
1	182.83	5.77			Primary carbide
2	206.89	5.12	172.46	5.20	Secondary carbide
3	138.03	5.28			Secondary carbide
4	351.86	2.78	351.86	2.78	Matrix (Ferrite)

Tab. 5 *Mechanical properties of ASP 2055 steel*

Position	Reduced Young's modulus of elasticity E_r [GPa]	Nanohardness H [GPa]	Diameter E_r	Diameter H	Estimated phase
0	212.50	9.96	207.80	5.14	Primary carbide
1	178.74	3.83			Primary carbide
2	232.17	1.64			Primary carbide
3	217.69	2.57	257.76	2.31	Matrix (Ferrite)
4	297.82	2.05			Matrix (Ferrite)

Tab. 6 *Comparison of steels phases, their nanohardness and reduced Young's modulus of elasticity*

Steel	Steel phase					
	Primary carbide		Secondary carbide		Matrix (Ferrite)	
	E_r [GPa]	H [GPa]	E_r [GPa]	H [GPa]	E_r [GPa]	H [GPa]
ASP 2017	172.86	6.09	172.46	5.20	351.86	2.78
ASP 2055	207.80	5.14			257.76	2.31

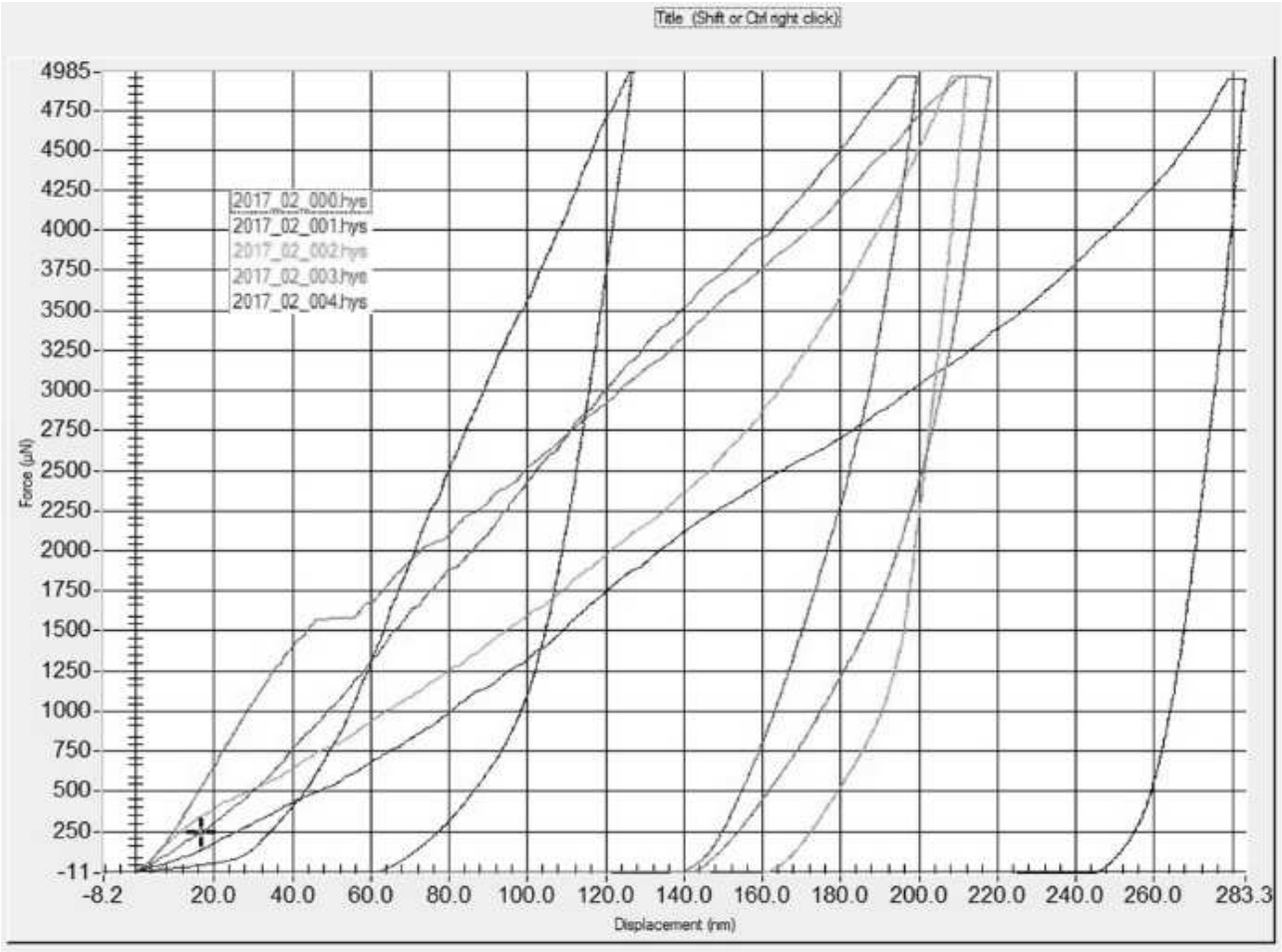

Fig. 9 *Nanoindentation curves for material ASP 2017*

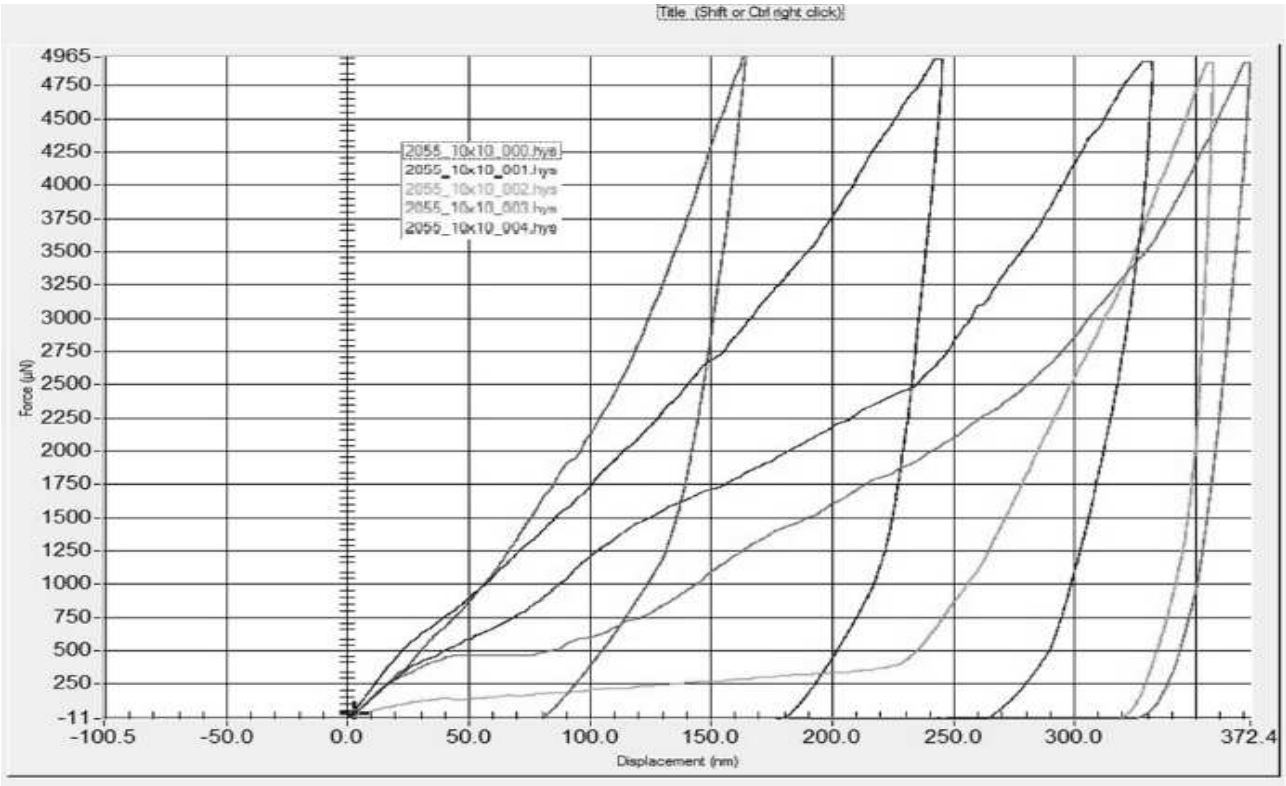

Fig. 10 *Nanoindentation curves for material ASP 2055*

For determination of numerical values of the nanohardness quantity is used nanoindentation the term Load curve. The second part of this curve, called Displacement, is used to determine the reduced Young's modulus of elasticity, as can be seen in (Fig. 9 and 10). A complete overview of the individual phases for high-speed steels ASP 2017 and ASP 2055, their nanohardness *H* and reduced modulus of elasticity *Er* can be found above in Tab. 4 and Tab. 5. Mutually graphical comparison according to the relation (1) of the obtained values of the Young's modulus of elasticity of the phase *Es* and also values of the reduced Young's modulus of elasticity *Er* obtained by quasi-static nanoindentation for ASP 2017 and ASP 2055 steels is shown in Fig. 11 and Fig. 12.

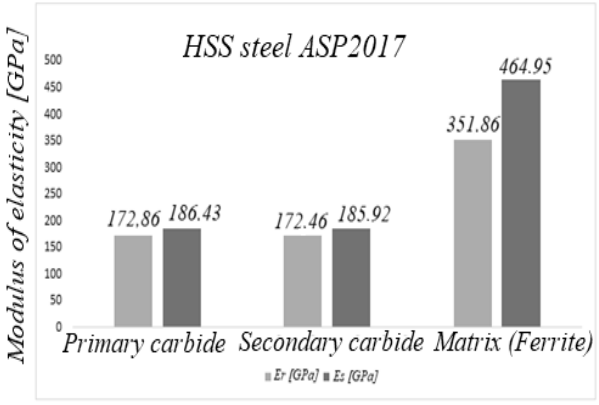

Fig. 11 *Graphical comparison of measured modulus Er and calculated modulus Es for ASP 2017*

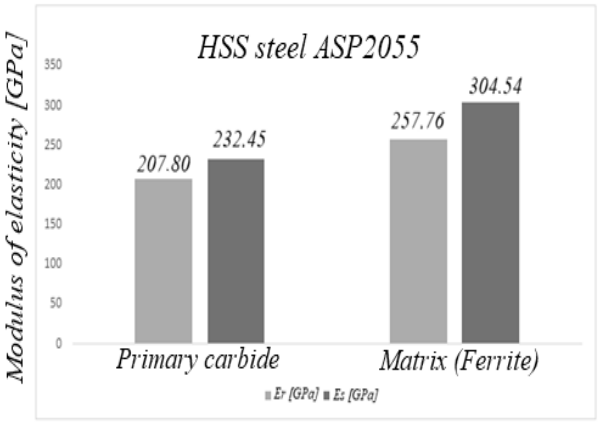

Fig. 12 *Graphical comparison of measured modulus Er and calculated modulus Es for ASP 2055*

4 Conclusions

The quasi-static nanoindentation of ASP 2017 and ASP 2055 steels is an initial phase of research for increasing of their properties. It helped to increase the knowledge about these two steels, but it is not enough to know the properties fully. Through standard microstructure and mechanical properties investigation procedures it is not possible to see standard grain borders, and also it is not possible to differentiate several phases or to define other material components. It is necessary to deeply investigate the tested steels by devices with higher magnification and display resolution. As a base for this following technique, quasi-static nanoindentation is altogether

with LO&SEM microscopy sufficient. Thanks to this part of research, it is possible to see very fine structure of these PM steels and to point out that their look and structure is different in comparison with standard way produced steels. The main goal of this research is a comprehensive advisement of the state of the microstructure of mentioned steels in the soft annealed state, as well as the nanomechanical properties of the microstructural components. The quasi-static nanoindentation was performed after the analysis through the SPM scanning. Further research will be focused on the aspect of the microstructure of the tested steels after heat treatment, as well as on the nanomechanical properties of the surface layers after the application of finishing machining methods. The following partial conclusions can be drawn from the conducted experiments:

- The microstructure of the ASP 2017 consists of larger primary carbides and smaller secondary carbides formed during annealing. Carbides are regularly distributed in the ferritic matrix
- The microstructure of the ASP 2055 consists of finely evenly distributed carbides in a ferritic matrix. The steel ASP2055 has high toughness because the formation of secondary carbides is suppressed
- Based on the measured results of the nanohardness *H* and the reduced Young's modulus of elasticity *Er* (see Tables 3 and 4), the individual observed phases of the investigated microstructures of both tested materials are defined as primary and secondary carbides, as well as the basic matrix formed by ferrite
- The calculations according to Equation 4, Table 3 shows a mutual comparison of measured reduced Young's modulus of elasticity with the calculated Young's modulus of elasticity of the examined phase. Comparison results with measured *Er* can also be seen graphically in Figs. 11 and 12
- All obtained results of the quasi-static nanoindentation analysis are in accordance with results & conclusions of investigations of other authors which examined similar materials
- Finally, it can be said that based on the implementation of the entire experiment, the methodology and parameters of quasi-static nanoindentation were proven, as well as experimentally verified values obtained by calculations

Acknowledgement

This publication was created within the implementation of the project "Development and support of research - development activities of the Center for Quality Testing and Diagnostics of Materials in the field of specialization RIS3 SK", ITMS2014 +: 313011W442, supported by the Operational Program Integrated Infrastructure and European Regional Development Fund.

References

[1] FISCHER – CRIPPS, A. C.: *Nanoindentation Springer Science (3rd edition)*, New York, ISBN – 13: 9781461429609, 2013

[2] OLIVER, W., PHARR, G. M: An improved technique for determining hardness and elastic modulus using load and displacement sensing indentation experiments, *Journal of Material Response*, Vol. 7 (1992), Issue 6, p. 1564-1583

[3] FISCHER-CRIPPS, A. C.: Critical review of analysis and interpretation of nanoindentation test data, *Surface and Coating Technology*, Vol. 200 (2006), p. 4153-4165

[4] WANG, S., ZHAO, H.: Low temperature nanoindentation: development and applications, *MDPI Micromachines*, Vol. 11 (2020), 25 p

[5] NAIMI-JAMAL, M. R., KAUPP, G.: Quantitative evaluation of nanoindents: do we need more reliable mechanical parameters for the characterization of materials? *International Journal of Materials Research*, Vol. 96 (2005), Issue 11, p. 1226-1236

[6] NGUYEN, V. L., KIM, E. A., YUN, J., CHOE, J., YANG, D. Y., LEE, CH. W., YU, J., H.: Nano-mechanical behavior of H13 tool steel fabricated by selective laser melting method, Metallurgical and material transactions A: *Physical metallurgy and material science* Vol. 50 (2019), Issue 2, p. 523-528

[7] NGUYEN, V. L., KIM, E. A., LEE, S. R., YUN, J. C., CHOE, J. H., YANG, D. Y., LEE, H. S., LEE, C. W., YU, J., H.: Evaluation of strain rate sensitivy of selective laser melted H13 tool steel using nanoindentation tests, *Metallurgical and material transactions A: Metals*, Vol. 8 (2018), p. 589

[8] MARASHI, J., YUKUSHINA, E., XIROUCHAKIS, P., ZANTE, R., FOSTER, J.: An evaluation of H13 tool steel deformation in hot forging conditions, *Journal of Material Processing Technology*, Vol. 246 (2017), p. 276-284

[9] LUONG NGUYEN, V., KIM, E., YUN, J., et al.: Evaluation of strain-rate sensitivity of selective laser melted H13 tool steel using nanoindentation tests, *Metals MDPI,* Vol. 8 (2018), p. 589-599

[10] YASAVOL, N., JAFARI, H.: Microstructure, mechanical and corrosion properties of friction stir-processed AISI D2 tool steel, *Journal of Materials Engineering and Performance*, Vol. 24 (2015), Issue 5, p. 2151-2157

[11] NURBANASARI, M., TSAKIROPOULOS, P., PALMIERE, E. J.: On the solidification of H23 tool steel*, Trans Indian Inst Met*, Vol. 67 (2014), Issue 6, p. 935-944

[12] BOUMAALI, B., NAIT ABDELLAH, Z., KEDDAM, M.: Characterization of bilayer (FeB/Fe_2B) in AISI H13 work tool steel. *Koroze a ochrana materiálu*, Vol. 65 (2021), Issue 2, p. 40-48

[13] MAJERÍK, J., BARÉNYI, I., SEDLÁK, J., KUSENDA, R., ECKERT, M.: Microstructural analysis of examined 33NiCrMoV15 steel and investigation of its nanomechanical properties after machining, *Manufacturing Technology*, Vol. 20 (2020), p. 72-77

[14] GROEB, M., FRITZ, M.: Process analysis on milled optical surfaces in hardened stainless steel*, Journal of Manufacturing and Materials Processing*, Vol. 67 (2019), Issue 3, 12 p

[15] NAGASHIMA, N., HAYKAWA, M., KIMURA, M.: Characterization of mechanical properties for ferritic heat-resisting steels (12Cr-2W) with different creep-fatigue properties by nanoindentation, *Materials Transactions*, Vol. 60 (2019), Issue 4, p. 495-502

[16] SU, J., TIAN, L., HU, R., LIU, H., FENG, T., WANG, J.: Effect of sputtering current on the comprehensive properties of (Ti, Al)N coating and high-speed steel substrate*, Journal of Materials Engineering and Performance*, Vol. 27 (2018), Issue 5, p. 2381-2387

[17] YAMAMOTO, M., TANAKA, M., FURUKIMI, O.: Hardness-deformation energy relationship in metals and alloys: a comparative evaluation based on nanoindentation testing and thermodynamic consideration, *MDPI Materials*, Vol. 14 (2021), 11 p

[18] LIU, Z., ZHANG, J., HE, B., ZOU, Y.: High speed nanoindentation mapping of a near-alpha titanium alloy made by additive manufacturing, *Journal of Materials Research*, Vol. 36 (2021), Issue 11, 12 p

[19] ZHU, Z., HUANG, H., LIU, J., YE, L., ZHU, Z.: Nanoindentation study on the creep characteristics and hardness of ion-irradiated alloys, *MDPI Materials*, Vol. 13 (2020), 12 p

[20] PÖHL, F., HARDES, C., SCHOLZ, F., FRENZEL, J.: Orientation dependent deformation behaviour of 316L steel manufactured by laser metal deposition and casting under local scratch and indentation load, *MDPI Materials*, Vol. 13 (2020), 19 p

[21] KLUČIAR, P., BARÉNYI, I., MAJERÍK, J.: Nanoindentation analysis of Inconel 625 alloy weld overlay on 16Mo3 steel, *Manufacturing Technology*, Vol. 22 (2022), Issue 1, p. 26-33

[22] BASAVARAJAPPA P. N., HEGDE, M. M. R., RAJENDRACHARI, S., SURENDRANATHAN, A. O.: Invsetigation of structural and mechanical properities of nanostructured TiMgSr alloy for biomedical applications, *Biointerface Research in Applied Chemistry*, Vol. 13 (2022), Issue 2, 12 p

[23] MENCIN, P., TYNE, C. J. V., LEVY, B. S.: A method for measuring the hardness of the surface layer on hot forging dies using a nanoindenter, *Journal of Material Engineering Performance*, Vol. 18 (2009), p. 1067-1072

[24] HAMID, A.: Deposition, microstructure and nanoindentation of multilayer Zr nitride and carbonitride nanostructured coatings, *Scientific reports*, Vol. 12 (2022), 16 p

[25] SVOBODOVÁ, J., LYSOŇKOVÁ, I., KREJČÍ, M.: Microhardness and nanohardness measurement of composite coatings applied to aluminium substrate, *Manufacturing Technology*, Vol. 19 (2019), Issue 4, p. 700-705

[26] GONZÁLES-HERNÁNDEZ, A., FLORES, M., MORALES, A. B., CAICEDO, J. C., DE SÁNCHEZ, N. A., BARRAGÁN RAMÍREZ, R..: Optical and tribo-mechanical characterization in metal-ceramic multilayer coatings*, Revista Mexicana de Física*, Vol. 66 (2020) Issue 4, p. 496-503

[27] PAUL, V., WAKEDA, M., AMEYAMA, K., OTA-KAWABATA, M., OHMURA, T.: Local deformation behaviour of the copper harmonic structure near grain boundaries investigated through nanoindentation, *MDPI Materials*, Vol. 14 (2021), 12 p

[28] OHMURA, T., WAKEDA, M..: Pop-in phenomenon as a fundamental plasticity probed by nanoindentation technique, *MDPI Materials*, Vol. 14 (2021), 30 p

[29] XIANG, S., YANG, X., LIANG, Y., WANG, L.: Texture evolution and nanohardness in Cu-Nb composite wires*, MDPI Materials*, Vol. 14 (2021), 12 p